Supplemental material to this article can be found at:
http://jpet.aspetjournals.org/content/suppl/2019/12/23/jpet.119.262063.DC1

1521-0103/372/3/331–338$35.00 https://doi.org/10.1124/jpet.119.262063
THE JOURNAL OF PHARMACOLOGY AND EXPERIMENTAL THERAPEUTICS J Pharmacol Exp Ther 372:331–338, March 2020

Relative Selectivity of Covalent Inhibitors Requires Assessment of Inactivation Kinetics and Cellular Occupancy: A Case Study of Ibrutinib and Acalabrutinib[S]

Melissa Hopper, Tarikere Gururaja, Taisei Kinoshita, James P. Dean, Ronald J. Hill, and Ann Mongan

Pharmacyclics LLC, an AbbVie Company, Sunnyvale, California

Received August 20, 2019; accepted December 11, 2019

ABSTRACT

Kinases form an attractive class of targets for small molecule inhibitors, but similarity among their adenosine triphosphate binding sites presents difficulties for developing selective drugs. Standard methods of evaluating selectivity of most reversibly bound drugs account for binding affinity but not the two-step process, affinity and inactivation, occurring during covalent inhibition. To illustrate this concept, we assessed the selectivity of Bruton's tyrosine kinase (BTK) over TEC kinases by two novel therapeutics: ibrutinib and acalabrutinib. The two-step process and time-dependent inhibition unique to covalent inhibitors were evaluated with two biochemical assays measuring enzymatic function and inhibition kinetics. The selectivity for BTK over TEC found in these biochemical analyses was 1–1.5 for ibrutinib and 3.0–4.2 for acalabrutinib. To further assess drug selectivity in a more physiologically relevant context, we developed cell-based occupancy assays that quantify the percentage of drug-inactivated kinases. Cellular selectivity of BTK over TEC was determined after MWCL-1 cells, and samples from patients with chronic lymphocytic leukemia (CLL) were treated for durations and concentrations based on human pharmacokinetics of each drug. In MWCL-1 cells, BTK/TEC selectivities measured at 0.5, 1, and 3 hours were 2.53, 1.05, and 1.51 for ibrutinib and 0.97, 1.13, and 2.56 for acalabrutinib, respectively. The equivalent selectivity measured in samples from patients with CLL were 1.31 ± 0.27 and 1.09 ± 0.11 for ibrutinib and acalabrutinib, respectively. Collectively, our data show that when properly accounting for time-dependent factors and relevant cellular context, ibrutinib and acalabrutinib demonstrate similar selectivity for BTK over TEC.

SIGNIFICANCE STATEMENT

This study shows relative selectivity of covalent inhibitors toward different kinase targets should be assessed with both affinity and inactivation kinetics to accurately account for time-dependent effects of covalent binding and assessed in a cellular matrix to reproduce the physiologic context of target inhibition. This is illustrated with a case study of ibrutinib and acalabrutinib for which selectivity assessment with appropriate assays, as opposed to measuring binding affinity with KINOME*scan* alone, corroborate emerging clinical data demonstrating similar safety profiles between the therapies.

Introduction

Bruton's tyrosine kinase (BTK), a member of the TEC family of kinases, mediates B-cell receptor signaling and has emerged over the past decade as an effective clinical target for first-line therapy and for treating relapsed/refractory chronic lymphocytic leukemia (CLL) (Stevenson et al., 2011; Woyach et al., 2012). Ibrutinib is the only once-daily BTK inhibitor that is approved in the United States, Europe, and other countries for the treatment of several B-cell malignancies, including CLL and mantle cell lymphoma (MCL) (). Acalabrutinib, another BTK inhibitor taken twice daily, has received conditional approval in the United States only for the treatment of relapsed/refractory MCL and is in development for the treatment of other B-cell malignancies (AstraZeneca Pharmaceuticals LP, 2017). Although it has been demonstrated that both ibrutinib and acalabrutinib potently inhibit BTK via covalent bond formation, selectivity for this target over other TEC family kinases has not been rigorously assessed.

In 2017, Barf and colleagues (2017) reported the pharmacology of acalabrutinib and highlighted its biochemical and cellular selectivity for BTK over other kinases in the TEC family. The authors used two different biochemical assays to assess the inhibition selectivity of BTK over TEC for several covalent BTK inhibitors, including ibrutinib and acalabrutinib. In their study, the potency for BTK was measured using the immobilized metal ion affinity-based fluorescence polarization (IMAP) assay, and the potency for TEC was measured using a time-resolved fluorescence resonance energy transfer

Financial support for this work was provided by Pharmacyclics LLC, an AbbVie Company.
This work was previously presented by M. Hopper et al. at the 60th ASH Annual Meeting and Exposition on December 1–4, 2018 (poster 3498).
Role of the Funder/Sponsor: Pharmacyclics LLC, an AbbVie Company, sponsored and designed the study. Study investigators and their research teams collected the data. The sponsor confirmed data accuracy and performed analysis of the data. Medical writing support was funded by the sponsor.
https://doi.org/10.1124/jpet.119.262063.
[S] This article has supplemental material available at jpet.aspetjournals.org.

ABBREVIATIONS: BTK, Bruton's tyrosine kinase; CLL, chronic lymphocytic leukemia; IMAP, immobilized metal ion affinity-based fluorescence polarization; PBMC, peripheral blood mononuclear cell; TR-FRET, time-resolved fluorescence resonance energy transfer.

(TR-FRET) assay. The two assays differed in that the IMAP assay informed enzymatic activity of the kinases, whereas the TR-FRET assay measured inhibition via competitive binding and thus only informed affinity. Neither of these assays was optimal for quantifying drug selectivity, because they assessed only part of the inactivation mechanism of action. Accordingly, although each assay reported higher potency for both BTK and TEC by ibrutinib relative to acalabrutinib, selectivity between the two kinases could not be inferred from the IC_{50} derived from the two different assay platforms. The authors further profiled inhibition via competitive binding of ibrutinib and acalabrutinib against a panel of 395 nonmutant human kinases using the KINOME*scan* Assay Platform (Eurofins DiscoverX Corporation, Fremont, CA). This experiment showed that when both drugs were tested at the same concentration, 1 μM, ibrutinib was more potent against BTK and TEC than acalabrutinib. Notably, physiologically relevant exposures for acalabrutinib are 5-fold higher than for ibrutinib (Byrd et al., 2013, 2016); although these results were consistent with earlier studies (Honigberg et al., 2010; Byrd et al., 2016) in finding ibrutinib as the more potent inhibitor, the arbitrary use of 1 μM resulted in data that were not informative toward understanding target inhibition of the two drugs at physiologically relevant exposures (Byrd et al., 2013, 2016).

Kinase inhibition via covalent bond formation is a two-step process that begins with the compound interacting with the kinase driven by affinity (represented by K_i) and ends with an inactivation step (K_{inact}). Accordingly, potency of covalent inhibitors cannot be determined using only traditional IC_{50} measurements because this does not account for the entirety of the two-step process of covalent bond formation (Bauer, 2015). Here, we used the ratio of K_{inact}/K_i, which is the preferred metric to rank potency of different covalent inhibitors against a target (Bauer, 2015). In fact, Barf and colleagues (2017) discussed the relevance of these two parameters in their article, highlighting the faster inactivation rate for an acrylamide-substituted acalabrutinib and higher target affinity by ibrutinib as the primary factors contributing to the difference in potency of each compound. Furthermore, both the IMAP and the TR-FRET platforms are biochemical assays that measure the enzymatic reactions in relatively artificial systems that do not account for the complexity of the cellular environment, which has high (millimolar) ATP concentrations and hundreds of protein interactions. Collectively, it is clear that selectivity can be accurately assessed only in a comprehensive manner, including analysis of binding kinetics, enzymatic activity, and cellular occupancy at physiologically relevant drug concentrations. In the present study, we assessed these three parameters to rigorously evaluate the selectivity of ibrutinib and acalabrutinib for BTK and TEC.

TABLE 1
BTK and TEC selectivity based on biochemical functional and kinetic analyses

Drug	IC_{50} (nM) ± S.D.		IC_{50} Ratio	K_i (nM) ± S.D.		K_{inact} (s^{-1}) ± S.D.		K_{inact}/K_i ($nM^{-1}*s^{-1}$) ± S.D.		Ratio of K_{inact}/K_i
	BTK	TEC	TEC/BTK	BTK	TEC	BTK	TEC	BTK	TEC	BTK/TEC
Ibrutinib	0.24 ± 0.2	0.24 ± 0.2	1	0.95 ± 0.009	1.8 ± 0.05	0.011 ± 0.0004	0.013 ± 0.0005	0.012 ± 0.0006	0.008 ± 0.0004	1.5
Acalabrutinib	2.3 ± 1.6	9.7 ± 2.6	4.2	8.7 ± 0.5	160 ± 37	0.0021 ± 0.0004	0.012 ± 0.001	0.00024 ± 0.00003	0.00008 ± 0.00001	3.0

Materials and Methods

Biochemical Assay—Enzymatic Function. Biochemical enzymatic IC_{50} data were generated by Nanosyn (Santa Clara, CA). Determination of inhibitor potency against BTK enzyme was carried out using the microfluidic-based LabChip 3000 Drug Discovery System (Caliper Life Sciences, Hopkinton, MA), which uses capillary electrophoresis to separate phosphorylated and nonphosphorylated peptides. Briefly, the enzyme reaction was started by preincubating

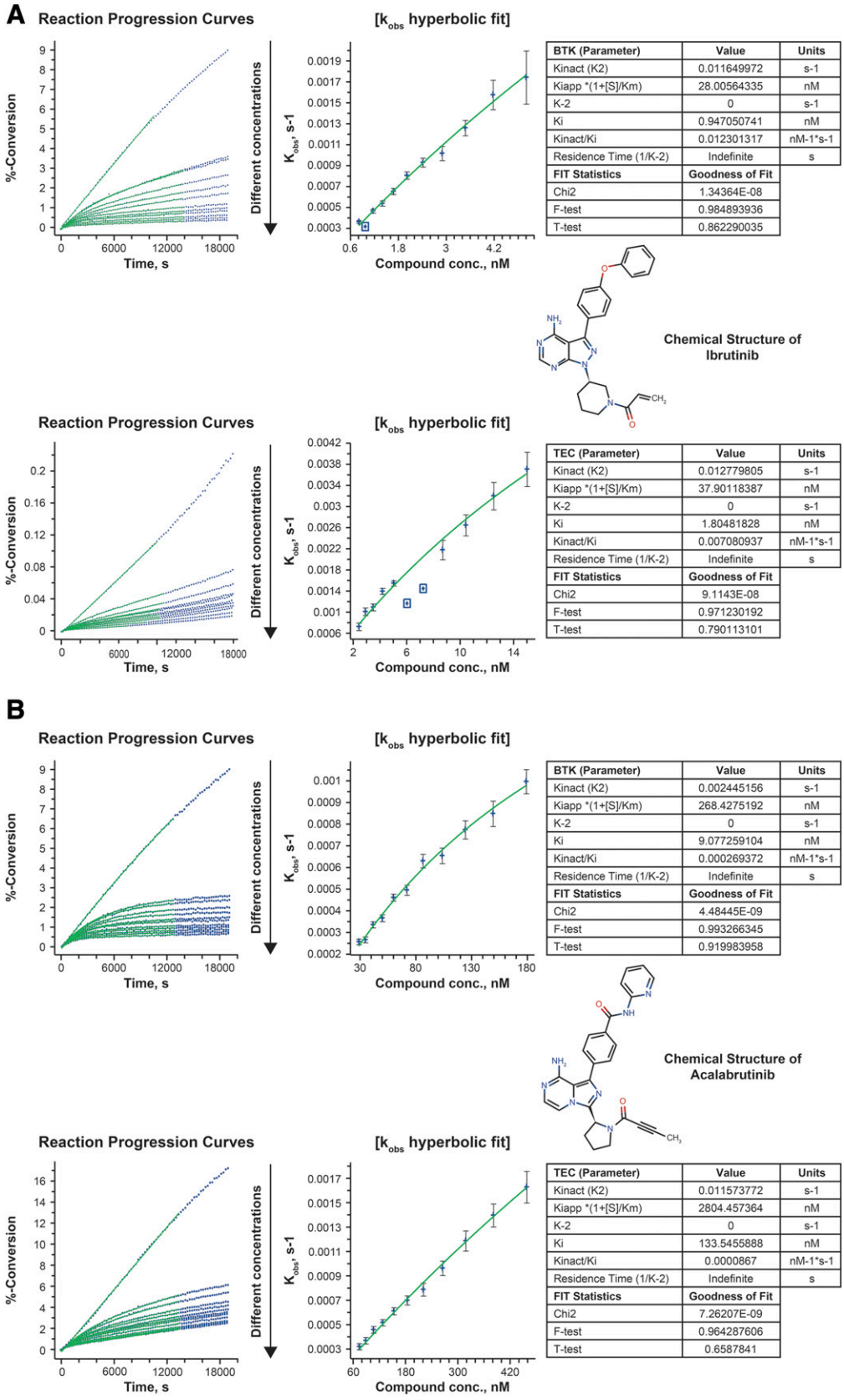

Fig. 1. Determination of BTK and TEC inactivation kinetic parameters for (A) ibrutinib and (B) acalabrutinib based upon time-dependent inhibition via reaction progression curves. k_{obs} (pseudo-first-order rate constant) was determined by the following equation: $k_{obs} = k{-}2 + k2*[I]/([I] + K_i*(1 + [S]/K_m))$, in which K_i* is the stable complex forming constant and K_i is the overall final inhibitory constant (for covalent irreversible inhibitors, $k2 = k_{inact}$ and $k{-}2 = 0$). Upon plotting concentration of inhibitor [I] vs. k_{obs}, goodness of fit parameters for the two drugs were determined using either hyperbolic or linear fit from the time-dependent inhibition equation: $[P] = Vs \times t + ((V_i - V_s)/K_{obs}) \times (1 - \exp(-K_{obs} \times t))$, in which V_i represents initial velocity, and V_s is final

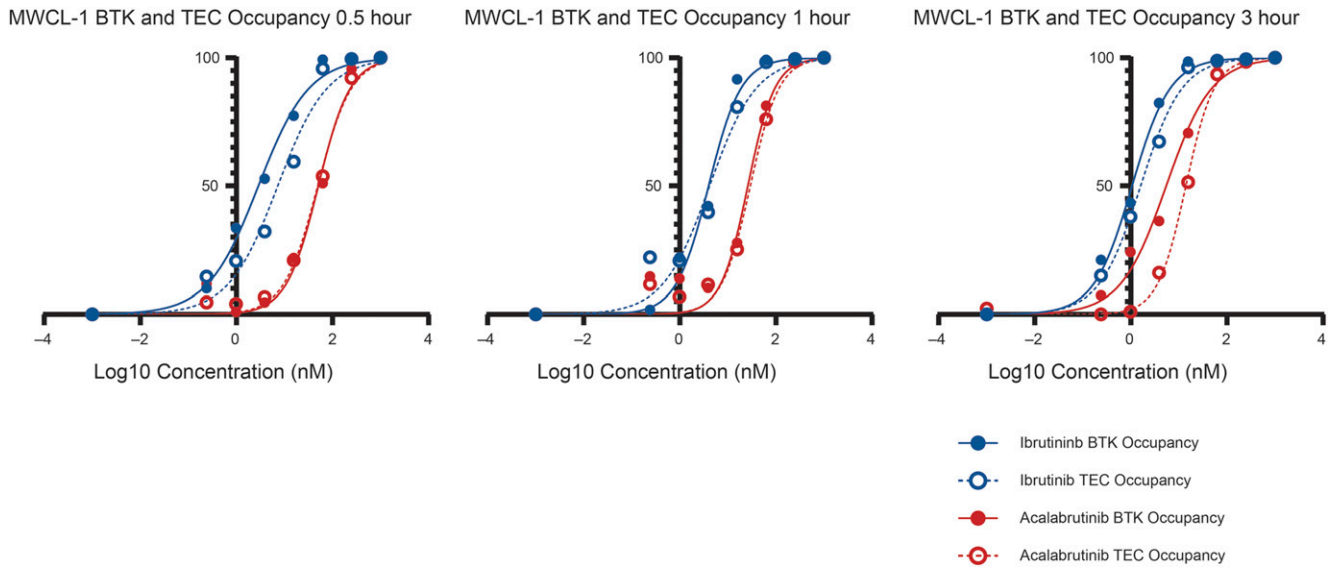

Fig. 2. Dose-response curves of BTK and TEC occupancy in the MWCL-1 cell line. BTK and TEC occupancy (closed and open circles) is shown for ibrutinib (blue lines) and acalabrutinib (red lines). Occupancy is shown for drug exposure at 0.5 hours (left), 1 hour (center), and 3 hours (right).

inhibitor at 12 different concentrations in DMSO (1000, 330, 110, 37, 12, 4.1, 1.4, 0.46, 0.15, 0.051, 0.017, and 0.006 nM) with purified BTK for 15 minutes in a buffer system consisting of 100 mM HEPES solution, pH 7.5, 0.1% bovine serum albumin, 0.01% Triton X-100 (Sigma-Aldrich, St. Louis, MO), 1 mM dithiothreitol, and 5 mM magnesium chloride at 25°C. After enzyme-inhibitor preincubation, the kinase reaction was initiated by adding peptide substrate and ATP (50 μM) prepared in the same assay buffer, followed by further incubation of reaction mixture for 3 hours. At the end of the incubation, the reaction was quenched by a buffer containing 50 mM of EDTA. Appropriate control samples (0% inhibition in the absence of inhibitor, DMSO only, and 100% inhibition in the absence of enzyme) were assembled in replicates of four and used to calculate the percentage of inhibition in the presence of compounds. IC_{50} values were determined by fitting the inhibition curves using a four-parameter sigmoidal dose-response model using XLfit 4 software (IDBS, Boston, MA). A similar protocol was used to determine the IC_{50} values for TEC kinase, with minor modifications to optimize for enzyme, peptide, and ATP concentrations.

Biochemical Assay—Kinetics of Target Inhibition. For kinetic studies, similar enzyme assay conditions were employed as described in the *Biochemical Assay—Enzymatic Function* section. The generation of progress curves for BTK/TEC peptide phosphorylation in the presence of test inhibitor was performed at 11 drug concentrations (10, 8.3, 6.9, 5.8, 4.8, 4.0, 3.4, 2.8, 2.3, 1.9, and 1.6 nM). After initiating the enzyme reaction, the real-time curves were obtained for a total period of 5 hours using a climate-controlled LabChip 3000 Drug Discovery System. Progress curves were then fitted by XLfit 4 software using the time-dependent inhibition equation $[P] = V_s \times t + ((V_i - V_s)/K_{obs}) \times (1 - \exp(-K_{obs} \times t))$, in which V_i is the initial velocity, V_s is the steady-state velocity, and K_{obs} represents the rate of inactivation. For time-dependent inhibitors, the obtained K_{obs} values were plotted against the compound concentration using either a hyperbolic or linear fit. The model with the better goodness of fit was selected. These plots enabled determination of K_{inact} and K_i values. The acquisition of all progress curve data points and the calculation of kinetic parameters were performed by Nanosyn.

Cell Treatments. The MWCL-1 cell line, which was established from a patient with Waldenström macroglobulinemia (Hodge et al., 2011), was obtained from Mayo Foundation for Medical Education and Research (Rochester, MN). MWCL-1 treatments were performed in six-well tissue culture plates using 6×10^6 cells per well at a concentration of 2×10^6 cells/ml in Gibco RPMI 1640 (ThermoFisher Scientific, Waltham, MA) supplemented with Gibco 1× Penicillin-Streptomycin (ThermoFisher Scientific), 10% heat-inactivated fetal bovine serum, and 1 mM Gibco Sodium Pyruvate (ThermoFisher Scientific). Cells were treated with inhibitors for 0.5, 1, or 3 hours at 37°C and 5% CO_2, with a final DMSO concentration of 0.1% (v/v). Following treatment, cells were washed two times with 1× PBS to remove excess compound. Cell pellets were lysed in 1× PBS with 0.1% NP-40 detergent and 1× Protease Inhibitor Cocktail (Sigma-Aldrich). Cell lysate protein concentrations were quantified by Pierce BCA Protein Assay (ThermoFisher Scientific) per manufacturer's instruction using a FlexStation 3 Multi-Mode Microplate Reader (Molecular Devices, San Jose, CA). Treatment-free cryopreserved CLL peripheral blood mononuclear cells (PBMCs) isolated from four donors were obtained from Discovery Life Sciences (Huntsville, AL). Samples were thawed, washed once with Gibco RPMI 1640 supplemented with 10% heat-inactivated fetal bovine serum, and resuspended in fresh medium. Cells were plated in a six-well tissue culture plate using 9×10^6 cells per well at a concentration of 3×10^6 cells/ml and incubated at 37°C with 5% CO_2 for 2 hours prior to compound treatment. Treatments and cell lysis were performed using the same procedure as was used for MWCL-1 cells.

Enzyme Occupancy Assays. Cell-based BTK and TEC occupancy assays were developed to evaluate drug selectivity between the two kinases in a more physiologically relevant system. An MSD Small Spot High Bind plate (Meso Scale Diagnostics, Rockville, MD) was coated with 35 μl of 10 μg/ml anti-TEC antibody (Sigma-Aldrich) or 35 μl of 1 μg/ml anti-BTK antibody and incubated overnight at 4°C. The following day, the plate was warmed to room temperature, washed three times with 200 μl of 1× MSD Tris Wash Buffer (Meso Scale Diagnostics), and blocked with 200 μl of 3% MSD Blocker A (Meso Scale Diagnostics) for 1 hour. In a 96-well plate, 25 μl of 2 mg/ml

steady-state velocity (for covalent irreversible inhibitors, $V_s = 0$). From the goodness of fit and statistical analysis data it is clear that the two drugs exhibited a hyperbolic fit (curve-fitting software XLfit4 yielded a goodness of fit with lower χ^2 values and F-Test greater than 0.95 in all the cases), indicating that the binding of the two drugs follows a two-step mechanism. The first step includes reversible binding of the inhibitor to the enzyme, which is followed by the second step of covalent bond formation for both BTK and TEC enzymes. Conc., concentration.

TABLE 2
IC_{50} derived from dose-response curves of BTK and TEC occupancy in the MWCL-1 cell line

Drug	Time Point (h)	BTK IC_{50} (nM)	TEC IC_{50} (nM)	BTK/TEC Selectivity[a]
Ibrutinib	0.5	2.88	7.28	2.53
	1	3.99	4.18	1.05
	3	1.06	1.60	1.51
Acalabrutinib	0.5	50.89	49.36	0.97
	1	26.10	29.38	1.13
	3	5.47	14.01	2.56

[a]BTK/TEC selectivity is defined as TEC IC_{50}/BTK IC_{50}.

cell lysate was incubated with 25 μl of 50 nM proprietary biotinylated probe for 1 hour to allow the probe to bind TEC or BTK kinase not occupied by drug. The MSD plate was then washed three times, and 45 μl of probe-labeled lysate was added to each well and incubated for 2 hours. The plate was then washed three times prior to the addition of 45 μl of MSD SULFO-TAG Streptavidin (Meso Scale Diagnostics) diluted 1:500 in 1× PBS. After 1 hour of incubation, 150 μl of 1× MSD Read Buffer (Meso Scale Diagnostics) was added to each well and the plate was read immediately on an MSD Sector S 600 plate reader (Meso Scale Diagnostics). Unless otherwise specified, incubation steps were performed at room temperature with 300 rpm shaking.

Results

Inhibition Kinetics of BTK and TEC by Ibrutinib and Acalabrutinib. Inhibition of kinases by covalent binding is a two-step process that is driven by affinity with the target followed by inactivation by covalent bond formation. Therefore, the assessment of relative selectivity toward different targets for covalent inhibitors should be evaluated using measurement of both binding affinity and time-dependent inactivation (Strelow, 2017). In the current study, biochemical analyses of enzymatic function were performed and kinetics measuring both of these parameters were derived using the LabChip 3000 Drug Discovery System. Biochemical IC_{50} values for kinase inhibition demonstrated BTK and TEC selectivity ratios of 1.0-fold for ibrutinib and 4.2-fold for acalabrutinib (Table 1). These data demonstrated similar binding affinity of ibrutinib for both BTK and TEC kinase, as indicated by their similar K_i values: 0.95 ± 0.009 nM (BTK) and 1.8 ± 0.05 nM (TEC) (Table 1). Examples of the enzymatic progression curves and hyperbolic fit curves that were used to calculate the kinetic parameters in Table 1 (K_i and K_{inact}) as well as the equations used for the calculations are shown in Fig. 1. The complete set of kinetic data for all determinations is included as Supplemental Material (Supplemental Figs. 1–8; Supplemental Tables 1–8). The rates of enzymatic inactivation (K_{inact}) of ibrutinib against both BTK and TEC were also similar: 0.011 ± 0.0004 (BTK) and 0.013 ± 0.0005 (TEC). In contrast, acalabrutinib demonstrated 20-fold higher binding affinity for BTK (8.7 ± 0.5) compared with TEC (160 ± 37) but a 5-fold faster rate of TEC inactivation (0.012 ± 0.001) compared with BTK inactivation (0.0021 ± 0.0004). Therefore, despite these large differences in binding and inactivation, selectivity for BTK over TEC, as measured by the K_{inact}/K_i ratio with this method, were within 2-fold for the two drugs: a selectivity ratio of 1.5 for ibrutinib and 3 for acalabrutinib (Table 1). This difference in kinetic properties of the two compounds highlights why different approaches are necessary to rank selectivity between reversible and covalent inhibitors. For reversible binding, relative selectivity can be inferred from the IC_{50} of affinity analysis alone because potency is driven by affinity in these cases. For covalent inhibitors, the IC_{50} does not reflect the combined affinity plus inactivation steps. The apparent IC_{50} for covalent inhibitors decreases as a function of time because of the depletion of active enzyme caused by covalent bond formation. Accordingly, this analysis demonstrated how binding affinity measured alone inadequately reflects selectivity among different targets of covalent inhibitors.

Acalabrutinib and Ibrutinib Exhibit Similar Selectivity for BTK Over TEC in MWCL-1 Cells and Human CLL PBMCs. MWCL-1 cells were treated with eight different

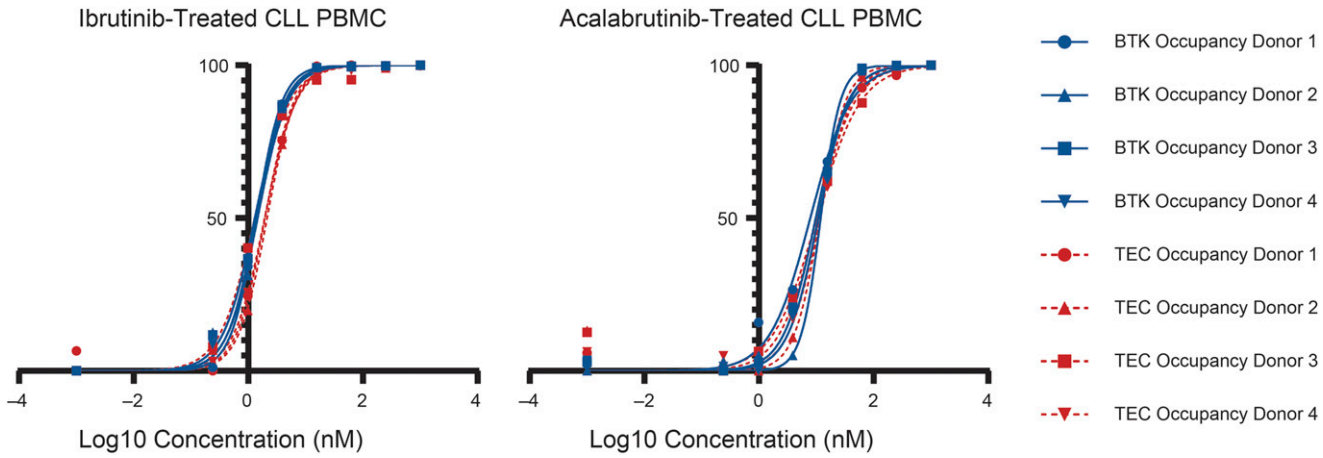

Fig. 3. Dose-response curves of BTK and TEC occupancy in human CLL PBMCs. Occupancy of BTK (blue lines) and TEC (red lines) is shown for human CLL PMBCs treated with ibrutinib (left) and acalabrutinib (right). Occupancy was assessed at 3 hours of exposure to ibrutinib or acalabrutinib.

TABLE 3
IC_{50} derived from dose-response curves of BTK and TEC occupancy in human CLL PBMCs

Drug	PBMC Donor	BTK IC_{50} (nM)	TEC IC_{50} (nM)	BTK/TEC Selectivity[a]	Mean ± S.D.
Ibrutinib	Donor 1	1.39	1.96	1.41	1.32 ± 0.27
	Donor 2	1.45	2.12	1.46	
	Donor 3	1.30	1.29	0.99	
	Donor 4	1.37	1.93	1.41	
Acalabrutinib	Donor 1	7.86	10.25	1.30	1.09 ± 0.11
	Donor 2	11.93	11.53	0.97	
	Donor 3	9.79	10.19	1.04	
	Donor 4	10.84	11.52	1.06	

[a]BTK/TEC selectivity is defined as TEC IC_{50}/BTK IC_{50}.

concentrations of either ibrutinib or acalabrutinib for 0.5, 1, and 3 hours (Fig. 2). The time points were selected to encompass the T_{max} (i.e., the time for drug to reach maximal plasma concentration in patients) of both compounds (Advani et al., 2013; Barf et al., 2017). With very short exposure (0.5 hours), ibrutinib showed slightly higher selectivity for BTK over TEC: when 50% of BTK was occupied, only 25% of TEC was occupied (Fig. 2, left). Acalabrutinib selectivity was not observed after 0.5-hour exposure (i.e., there was no separation for BTK and TEC dose-response curves). BTK over TEC selectivity was minimal for both drugs with 1-hour exposure (Fig. 2, center) across eight concentrations. With 3 hours of treatment, there was modest selectivity indicated by the small separation between the BTK and TEC dose-response curves for both drugs (Fig. 2, right), and this selectivity was nearly equivalent for both drugs. In effect, these cellular results are consistent with the biochemical results; ibrutinib exhibited slightly higher potency on BTK over TEC at 0.5 hours, but similar potency against the two kinases became apparent with longer treatment time (Table 2). The time-dependent effect of kinase inhibition observed here is not unlike the physiologic activities of these drugs in vivo. Because the drug-binding reaction is irreversible, the amount of drug-bound targets increases with longer duration of exposure. The current data with MWCL-1 cells show that the two drugs have nearly equivalent selectivity between BTK and TEC, and the ranges of selectivity ratios (BTK/TEC) were similarly small (1.05–2.53 and 0.97–2.56 for ibrutinib and acalabrutinib, respectively) throughout the time window of 0.5–3 hours (Table 2) that is required to achieve maximum occupancy resulting in target inhibition (Barf et al., 2017). Protein content and cellular compositions of PBMCs from patients with CLL may differ from those of the MWCL-1 cells, so we further evaluated the differential selectivity of the two drugs in cryopreserved PBMCs isolated from patients with CLL who were previously untreated. Cellular occupancy assays, which measure the percentage of target kinases bound by drugs, were conducted after each patient sample was treated with either ibrutinib or acalabrutinib for 3 hours (Fig. 3). Despite the potential biological variation among different donors, IC_{50} values against BTK and TEC were highly similar for both drugs across four individual patients (Table 3). Ibrutinib was more potent toward both kinases, with IC_{50} for BTK ranging from 1.3 to 1.5 nM and TEC ranging from 1.3 to 2.1 nM. Acalabrutinib was approximately 10-fold less potent against both kinases, with IC_{50} for BTK ranging from 7.9 to 11.9 nM and TEC ranging from 10.2 to 11.5 nM. Results of this occupancy assay are consistent with findings from biochemical analyses from the present study and others' work (Bye et al., 2015); ibrutinib is generally a more potent compound than acalabrutinib toward members of the TEC kinase family. However, as observed in MWCL-1 cells, the two drugs' BTK/TEC selectivity ratios observed in samples from patients with CLL were remarkably similar: 1.32 ± 0.27 for ibrutinib and 1.09 ± 0.11 for acalabrutinib (Table 3). These data indicate that the two compounds exerted equivalent selectivity for BTK over TEC in a cellular environment despite having the higher potency of ibrutinib against BTK and TEC kinases based on IC_{50} values (Fig. 4; Table 3). In general, the implication of higher potency is that a drug is more reactive toward its targets and less drug is needed to achieve pharmacologic activity, whereas selectivity is a measure of the ratio of on-target/off-target effects, such as BTK over TEC. Here, the collective data indicate that ibrutinib is a more

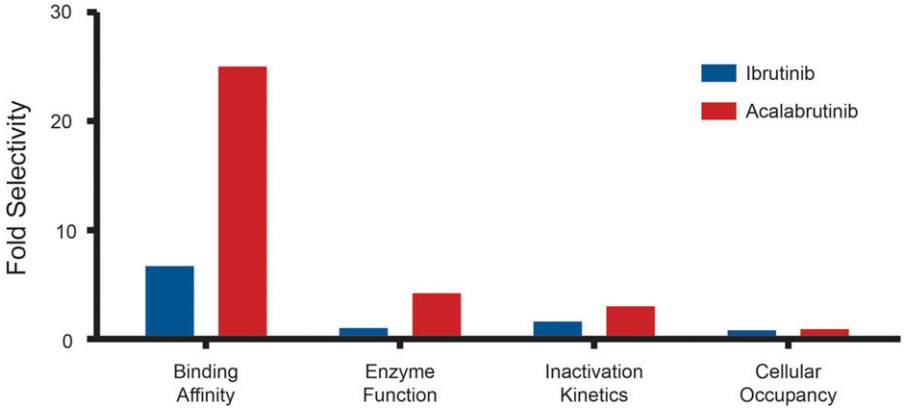

Fig. 4. Apparent selectivity of ibrutinib and acalabrutinib. Binding affinity data are reported by Barf et al. (2017). Enzyme function assay data are the IC_{50} ratios of TEC/BTK, and inactivation kinetics data are the K_{inact}/K_i ratios for ibrutinib (blue) and acalabrutinib (red). Cellular occupancy data are mean TEC/BTK selectivity measured by IC_{50} ratio for human CLL PMBCs.

potent drug than acalabrutinib toward its targets, but acalabrutinib does not offer improved on-target/off-target selectivity.

Discussion

Kinases form an attractive target class for small molecule inhibitors. Specifically, targeting BTK has resulted in therapies for numerous hematologic malignancies that previously had substantial unmet medical needs. However, the high similarity of the ATP binding site on protein kinases, a typical target of inhibition, mounts a continuous challenge for developing selective small molecule inhibitors for this target class. Our understanding of the selectivity of covalent and noncovalent inhibitors is highly dependent on the assessment methods, which have different implications and interpretations for irreversible and reversible binding modes. Crucial to this is the understanding that covalent kinase inhibition is a two-step process involving initial binding (driven by affinity) and time-dependent inactivation (driven by covalent bond formation). Thus, to evaluate biochemical potency and understand target selectivity of covalent inhibitors, both steps must be evaluated.

Published pharmacokinetics for ibrutinib and acalabrutinib report that the two compounds reach peak plasma concentrations between 1 and 2 hours and between 0.6 and 1.1 hours after dosing, respectively (Advani et al., 2013; Byrd et al., 2016). In a recent pharmacokinetic/pharmacodynamic modeling study of a covalent BTK inhibitor, it was shown that target occupancy in B cells and drug plasma exposure reach peak levels at the same time points (Daryaee et al., 2017). C_{max} for ibrutinib at 420 mg once daily (310 nM) was significantly lower than that of acalabrutinib at 100 mg twice daily (1.78 μM) (Byrd et al., 2016; Chen et al., 2018). These data show that direct comparison between the two drugs using in vitro systems should be conducted at concentrations consistent with this 5-fold or greater difference in human exposure levels. Without such considerations, the physiologic effects of these agents cannot be reasonably discerned. In one example of such oversight, Bye and colleagues (2015) argued that acalabrutinib is a less potent inhibitor of TEC phosphorylation based on in vitro analysis using equal concentration of either drug but subsequently discovered that therapeutic doses of acalabrutinib did inhibit TEC based on their own findings from patient samples (Bye et al., 2015)(). These authors concluded that the apparent potency of acalabrutinib toward both BTK and TEC in their in vitro experiments was lower than that observed in patients, because blood samples derived from patients treated with ibrutinib and acalabrutinib exhibited very similar platelet aggregation responses. These inconsistencies highlight the importance of adjusting in vitro exposure according to a drug's therapeutic concentration to obtain experimental results that are informative toward understanding the drug's effects in humans.

The recent high interest in understanding kinase selectivity profiles of various BTK inhibitors stems from a desire to optimize patient outcomes with treatment, minimize adverse events, and understand how off-target effects may be related to such events. For example, bleeding is an adverse event observed in patients treated with BTK inhibitors, with most cases being grade 1 or 2 in severity (Mock et al., 2018). Although clinical data were still being accumulated, an earlier hypothesis based on kinase affinity data proposed that acalabrutinib might lead to lower bleeding rates because of its higher selectivity for BTK relative to TEC (Byrd et al., 2016; Barf et al., 2017; Awan et al., 2019). However, when properly adjusted for clinical exposure, covalent binding mechanism, and enzymatic activity, our data and those of other groups (Bye et al., 2017) now indicate that ibrutinib and acalabrutinib have similar selectivity between BTK and TEC. This similar selectivity is consistent with a recent study suggesting that platelet inhibition and potential hemorrhagic risk predicted by in vitro closure time are likelyclass effects across five BTK inhibitors: ibrutinib, zanubrutinib, acalabrutinib, tirabrutinib, and evobrutinib (Denzinger et al., 2019). Furthermore, recent mechanistic investigations of the effects of ibrutinib and acalabrutinib on platelet functions suggested that polymorphism of drug efflux pumps might sensitize some patients toward platelet aggregation impairment more than others (Series et al., 2019). Because polymorphism in drug efflux pumps is an intrinsic factor, platelet aggregation did not improve when the authors retreated the same patient samples with acalabrutinib. Emerging clinical data now increasingly indicate that the bleeding rates of ibrutinib and acalabrutinib are similar, with more bleeding events reported for patients treated with acalabrutinib; 60% of 99 patients treated with first-line acalabrutinib reported bleeding events of all grades, and two of these patients showed grade 3 events after longer follow-up (median time on study of 33 months) (Byrd et al., 2018).

In summary, our study applies fundamental biochemistry principles to demonstrate how standard methods used to evaluate target selectivity for reversible inhibitors fail to fully characterize irreversible inhibitor selectivity. The current case study of the two covalent inhibitors ibrutinib and acalabrutinib highlights how these results, when performed at physiologic concentrations and in a more relevant cellular context, better inform the understanding of possible off-target clinical observations of bleeding events with these two drugs.

Acknowledgments

We thank Sany Hoxha for generation of figures and Jo Bairzin for medical writing, which was supported by Pharmacyclics LLC, an AbbVie Company.

Authorship Contributions

Participated in research design: Gururaja, Kinoshita, Hill, Mongan.

Conducted experiments: Hopper, Gururaja.

Contributed new reagents or analytic tools: Hopper.

Performed data analysis: Hopper, Gururaja, Hill, Mongan.

Wrote or contributed to the writing of the manuscript: Hopper, Gururaja, Kinoshita, Dean, Hill, Mongan.

References

Advani RH, Buggy JJ, Sharman JP, Smith SM, Boyd TE, Grant B, Kolibaba KS, Furman RR, Rodriguez S, Chang BY, et al. (2013) Bruton tyrosine kinase inhibitor ibrutinib (PCI-32765) has significant activity in patients with relapsed/refractory B-cell malignancies. *J Clin Oncol* **31**:88–94.

AstraZeneca Pharmaceuticals LP (2017) *CALQUENCE (acalabrutinib) capsules, for oral use*, AstraZeneca Pharmaceuticals LP, Wilmington, DE.

Awan FT, Schuh A, Brown JR, Furman RR, Pagel JM, Hillmen P, Stephens DM, Woyach J, Bibikova E, Charuworn P, et al. (2019) Acalabrutinib monotherapy in patients with chronic lymphocytic leukemia who are intolerant to ibrutinib. *Blood Adv* **3**:1553–1562.

Barf T, Covey T, Izumi R, van de Kar B, Gulrajani M, van Lith B, van Hoek M, de Zwart E, Mittag D, Demont D, et al. (2017) Acalabrutinib (ACP-196): a covalent Bruton tyrosine kinase inhibitor with a differentiated selectivity and in vivo potency profile. *J Pharmacol Exp Ther* **363**:240–252.

Bauer RA (2015) Covalent inhibitors in drug discovery: from accidental discoveries to avoided liabilities and designed therapies. *Drug Discov Today* **20**:1061–1073.

Bye AP, Unsworth AJ, Desborough MJ, Hildyard CAT, Appleby N, Bruce D, Kriek N, Nock SH, Sage T, Hughes CE, et al. (2017) Severe platelet dysfunction in NHL patients receiving ibrutinib is absent in patients receiving acalabrutinib. *Blood Adv* **1**:2610–2623.

Bye AP, Unsworth AJ, Vaiyapuri S, Stainer AR, Fry MJ, and Gibbins JM (2015) Ibrutinib inhibits platelet integrin αIIbβ3 outside-in signaling and thrombus stability but not adhesion to collagen. *Arterioscler Thromb Vasc Biol* **35**: 2326–2335.

Byrd JC, Furman RR, Coutre SE, Flinn IW, Burger JA, Blum KA, Grant B, Sharman JP, Coleman M, Wierda WG, et al. (2013) Targeting BTK with ibrutinib in relapsed chronic lymphocytic leukemia. *N Engl J Med* **369**:32–42.

Byrd JC, Harrington B, O'Brien S, Jones JA, Schuh A, Devereux S, Chaves J, Wierda WG, Awan FT, Brown JR, et al. (2016) Acalabrutinib (ACP-196) in relapsed chronic lymphocytic leukemia. *N Engl J Med* **374**:323–332.

Byrd JC, Woyach JA, Furman RR, Martin P, Brien SM, Brown JR, Stephens DM, Barrientos JC, Devereux S, Hillmen P, et al. (2018) Acalabrutinib in treatment-naive (TN) chronic lymphocytic leukemia (CLL): updated results from the phase 1/2 ACE-CL-001 study. *Blood* **132**:692.

Chen J, Kinoshita T, Gururaja T, Sukbuntherng J, James D, Lu D, Whang J, Versele M, and Chang BY (2018) The effect of Bruton's tyrosine kinase (BTK) inhibitors on collagen-induced platelet aggregation, BTK, and tyrosine kinase expressed in hepatocellular carcinoma (TEC). *Eur J Haematol* DOI: 10.1111/ejh.13148 [published ahead of print].

Daryaee F, Zhang Z, Gogarty KR, Li Y, Merino J, Fisher SL, and Tonge PJ (2017) A quantitative mechanistic PK/PD model directly connects Btk target engagement and *in vivo* efficacy. *Chem Sci (Camb)* **8**:3434–3443.

Denzinger V, Busygina K, Jamasbi J, Pekrul I, Spannagl M, Weber C, Lorenz R, and Siess W (2019) Optimizing platelet GPVI inhibition versus haemostatic impairment by the Btk inhibitors ibrutinib, acalabrutinib, ONO/GS-4059, BGB-3111 and evobrutinib. *Thromb Haemost* **119**:397–406.

Hodge LS, Novak AJ, Grote DM, Braggio E, Ketterling RP, Manske MK, Price Troska TL, Ziesmer SC, Fonseca R, Witzig TE, et al. (2011) Establishment and characterization of a novel Waldenstrom macroglobulinemia cell line, MWCL-1. *Blood* **117**:e190–e197.

Honigberg LA, Smith AM, Sirisawad M, Verner E, Loury D, Chang B, Li S, Pan Z, Thamm DH, Miller RA, et al. (2010) The Bruton tyrosine kinase inhibitor PCI-32765 blocks B-cell activation and is efficacious in models of autoimmune disease and B-cell malignancy. *Proc Natl Acad Sci USA* **107**:13075–13080.

Janssen-Cilag International NV (2018) IMBRUVICA (ibrutinib) summary of product characteristics, Janssen-Cilag International NV, Beerse, Belgium.

Mock J, Kunk PR, Palkimas S, Sen JM, Devitt M, Horton B, Portell CA, Williams ME, and Maitland H (2018) Risk of major bleeding with ibrutinib. *Clin Lymphoma Myeloma Leuk* **18**:755–761.

Pharmacyclics LLC (2019) *IMBRUVICA (ibrutinib) prescribing information*, Pharmacyclics LLC, Sunnyvale, CA.

Series J, Garcia C, Levade M, Viaud J, Sié P, Ysebaert L, and Payrastre B (2019) Differences and similarities in the effects of ibrutinib and acalabrutinib on platelet functions. *Haematologica* **104**:2292–2299.

Stevenson FK, Krysov S, Davies AJ, Steele AJ, and Packham G (2011) B-cell receptor signaling in chronic lymphocytic leukemia. *Blood* **118**:4313–4320.

Strelow JM (2017) A perspective on the kinetics of covalent and irreversible inhibition [published correction appears in SLAS Discov (2017) 22:652]. *SLAS Discov* **22**:3–20.

Woyach JA, Johnson AJ, and Byrd JC (2012) The B-cell receptor signaling pathway as a therapeutic target in CLL. *Blood* **120**:1175–1184.

Address correspondence to: Ann Mongan, Pharmacyclics, LLC, 999 E. Arques Avenue, Sunnyvale, CA 94085. E-mail: amongan@pcyc.com

Supplemental Information.

Relative Selectivity of Covalent Inhibitors Requires Assessment of Inactivation Kinetics and Cellular Occupancy: A Case Study of Ibrutinib and Acalabrutinib

Melissa Hopper, Tarikere Gururaja, Taisei Kinoshita, James P. Dean, Ronald J. Hill, Ann Mongan

Journal of Pharmacology and Experimental Therapeutics

Supplemental Table 1. BTK enzyme kinetics data for ibrutinib (0.35 nM BTK)

Compound	Enzyme	Enzyme concentration, nM	ATP concentration, uM	Compound concentration, nM	K_{obs}, s-1	95%-confidence
Ibrutinib	BTK	0.35	1000	10	0.002622204	0.000360793
Ibrutinib	BTK	0.35	1000	8.333333333	0.002546468	0.000330995
Ibrutinib	BTK	0.35	1000	6.944444444	0.002405458	0.000221326
Ibrutinib	BTK	0.35	1000	5.787037037	0.001744919	0.000127889
Ibrutinib	BTK	0.35	1000	4.822530864	0.00177236	0.000185465
Ibrutinib	BTK	0.35	1000	4.01877572	0.001146117	0.000100137
Ibrutinib	BTK	0.35	1000	3.348979767	0.000984421	4.18082E-05
Ibrutinib	BTK	0.35	1000	2.790816472	0.000909377	3.23242E-05
Ibrutinib	BTK	0.35	1000	2.325680394	0.000821419	2.85424E-05
Ibrutinib	BTK	0.35	1000	1.938066995	0.00067625	2.23957E-05
Ibrutinib	BTK	0.35	1000	1.615055829	0.000610541	4.48376E-05

Supplemental Figure 1. BTK enzyme kinetics plots for ibrutinib (1)

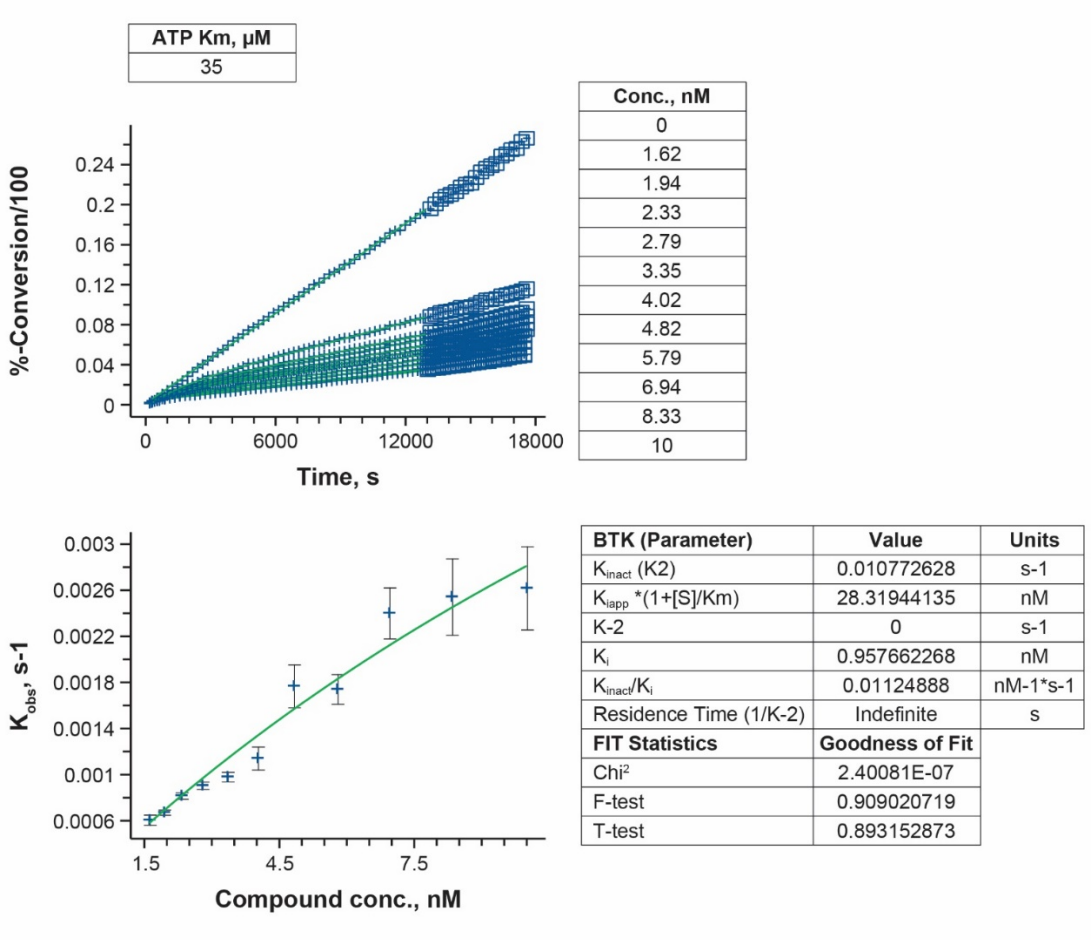

BTK (Parameter)	Value	Units
K_{inact} (K2)	0.010772628	s-1
K_{iapp} *(1+[S]/Km)	28.31944135	nM
K-2	0	s-1
K_i	0.957662268	nM
K_{inact}/K_i	0.01124888	nM-1*s-1
Residence Time (1/K-2)	Indefinite	s
FIT Statistics	**Goodness of Fit**	
Chi^2	2.40081E-07	
F-test	0.909020719	
T-test	0.893152873	

Supplemental Table 2. BTK enzyme kinetics data for ibrutinib (0.045 nM BTK)

Compound	Enzyme	Enzyme concentration, nM	ATP concentration, uM	Compound concentration, nM	K_{obs}, s-1	95%-confidence
Ibrutinib	BTK	0.045	1000	5	0.001745425	0.000253643
Ibrutinib	BTK	0.045	1000	4.166666667	0.001578286	0.000140563
Ibrutinib	BTK	0.045	1000	3.472222222	0.00126266	7.3267E-05
Ibrutinib	BTK	0.045	1000	2.893518519	0.001018874	6.78472E-05
Ibrutinib	BTK	0.045	1000	2.411265432	0.000931715	4.25298E-05
Ibrutinib	BTK	0.045	1000	2.00938786	0.000808285	3.47423E-05
Ibrutinib	BTK	0.045	1000	1.674489883	0.000656164	2.93531E-05
Ibrutinib	BTK	0.045	1000	1.395408236	0.00054087	2.39779E-05
Ibrutinib	BTK	0.045	1000	1.162840197	0.000468612	1.93592E-05
Ibrutinib	BTK	0.045	1000	0.969033497	0.000317853	1.73319E-05
Ibrutinib	BTK	0.045	1000	0.807527914	0.000365215	1.46379E-05

Supplemental Figure 2. BTK kinetics plots for ibrutinib (2)

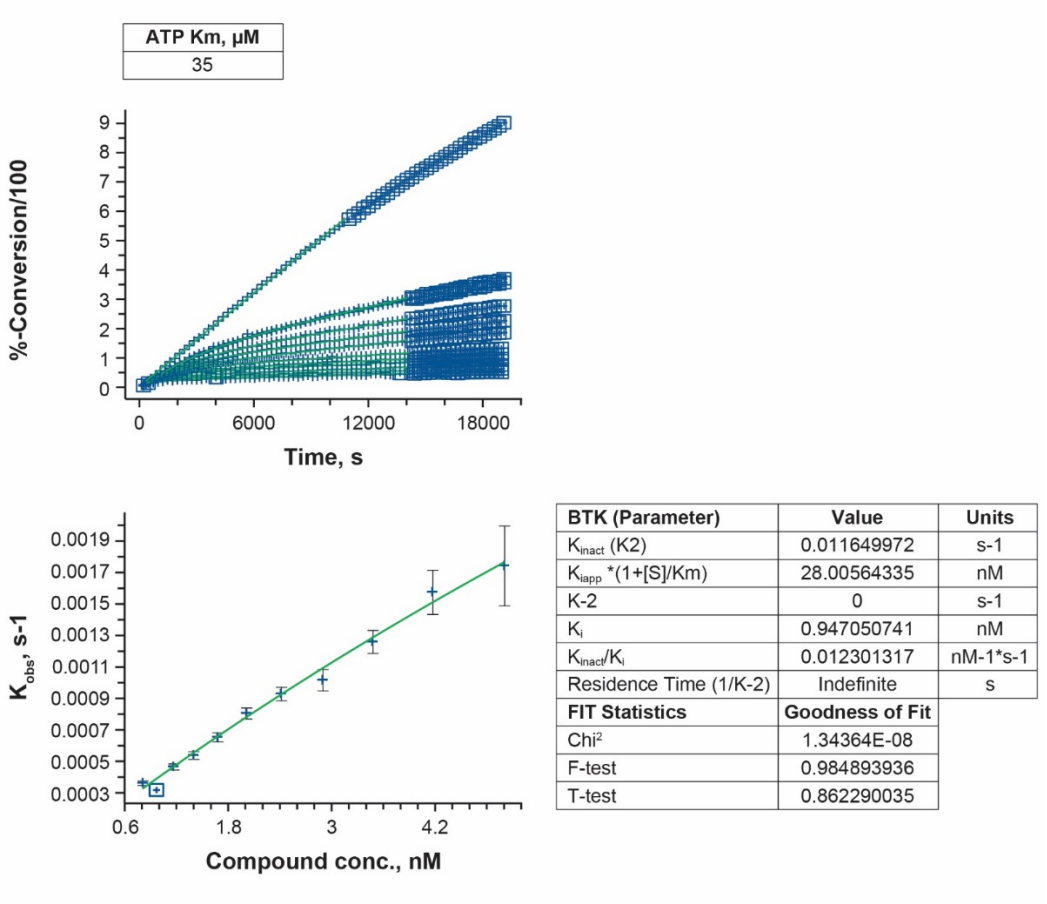

BTK (Parameter)	Value	Units
K_{inact} (K2)	0.011649972	s-1
K_{iapp} *(1+[S]/Km)	28.00564335	nM
K-2	0	s-1
K_i	0.947050741	nM
K_{inact}/K_i	0.012301317	nM-1*s-1
Residence Time (1/K-2)	Indefinite	s
FIT Statistics	**Goodness of Fit**	
Chi^2	1.34364E-08	
F-test	0.984893936	
T-test	0.862290035	

Supplemental Table 3. BTK enzyme kinetics data for acalabrutinib (0.35 nM BTK)

Compound	Enzyme	Enzyme concentration, nM	ATP concentration, uM	Compound concentration, nM	K_{obs}, s-1	95%-confidence
Acalabrutinib	BTK	0.35	1000	321.97	0.00097791	3.61277E-05
Acalabrutinib	BTK	0.35	1000	268.3083333	0.000956686	3.22938E-05
Acalabrutinib	BTK	0.35	1000	223.5902778	0.000907469	3.34095E-05
Acalabrutinib	BTK	0.35	1000	186.3252315	0.000846832	2.59687E-05
Acalabrutinib	BTK	0.35	1000	155.2710262	0.000714928	2.19069E-05
Acalabrutinib	BTK	0.35	1000	129.3925219	0.000692553	3.28869E-05
Acalabrutinib	BTK	0.35	1000	107.8271016	0.000487165	1.9903E-05
Acalabrutinib	BTK	0.35	1000	89.85591796	0.000462368	1.87039E-05
Acalabrutinib	BTK	0.35	1000	74.87993163	0.000420859	1.36238E-05
Acalabrutinib	BTK	0.35	1000	62.39994303	0.000367365	1.18944E-05
Acalabrutinib	BTK	0.35	1000	51.99995252	0.000290036	7.58079E-06

Supplemental Figure 3. BTK enzyme kinetics plots for acalabrutinib (1)

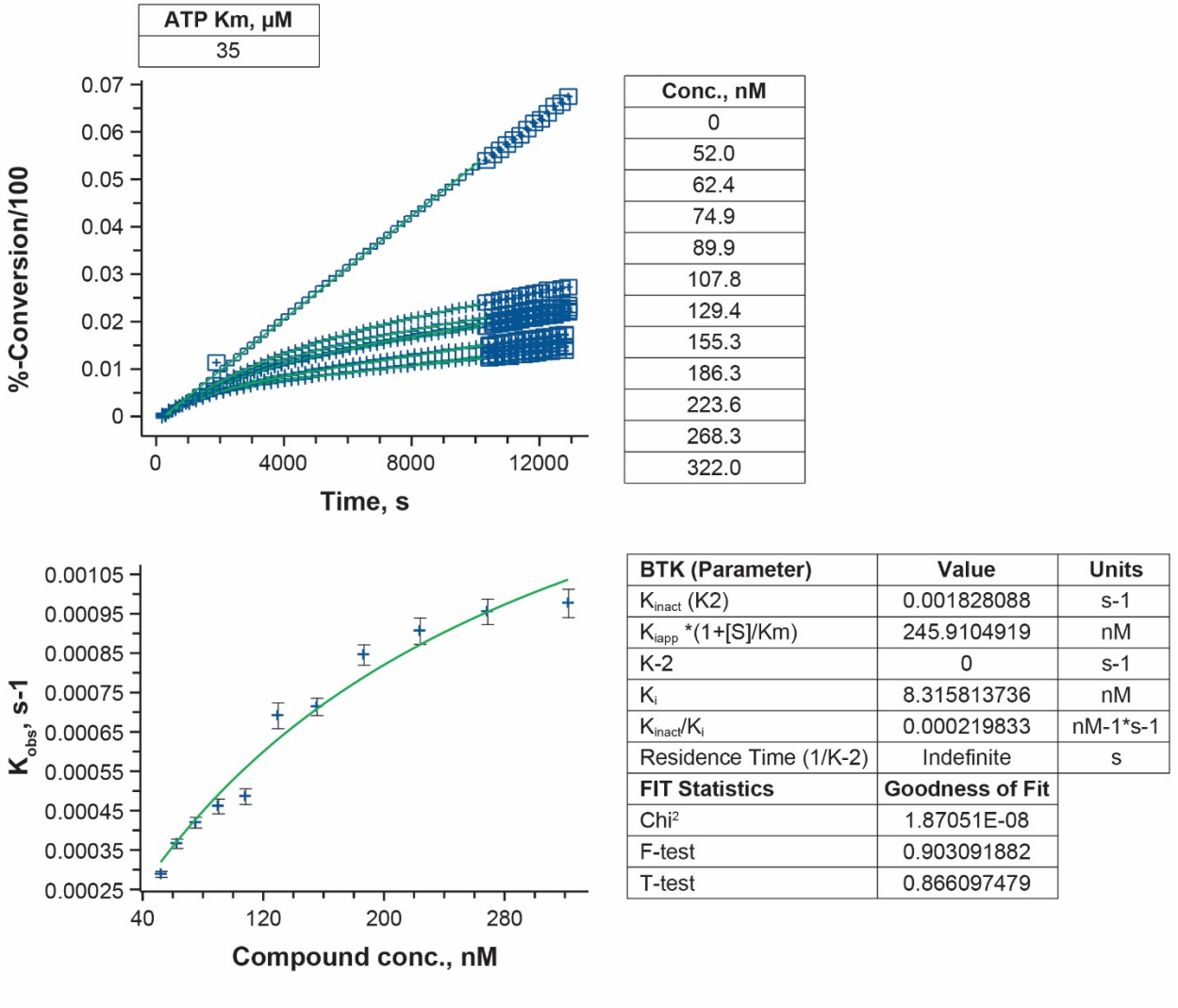

Conc., nM
0
52.0
62.4
74.9
89.9
107.8
129.4
155.3
186.3
223.6
268.3
322.0

BTK (Parameter)	Value	Units
K_{inact} (K2)	0.001828088	s-1
K_{iapp} *(1+[S]/Km)	245.9104919	nM
K-2	0	s-1
K_i	8.315813736	nM
K_{inact}/K_i	0.000219833	nM-1*s-1
Residence Time (1/K-2)	Indefinite	s
FIT Statistics	**Goodness of Fit**	
Chi^2	1.87051E-08	
F-test	0.903091882	
T-test	0.866097479	

Supplemental Table 4. BTK enzyme kinetics data for acalabrutinib (0.045 nM BTK)

Compound	Enzyme	Enzyme concentration, nM	ATP concentration, uM	Compound concentration nM	K_{obs}, s-1	95%-confidence
Acalabrutinib	BTK	0.045	1000	178.9	0.000997718	5.57243E-05
Acalabrutinib	BTK	0.045	1000	149.0833333	0.000849673	5.84386E-05
Acalabrutinib	BTK	0.045	1000	124.2361111	0.000775032	4.21489E-05
Acalabrutinib	BTK	0.045	1000	103.5300926	0.000655515	3.59637E-05
Acalabrutinib	BTK	0.045	1000	86.27507716	0.000631197	3.11489E-05
Acalabrutinib	BTK	0.045	1000	71.89589763	0.000496656	2.36196E-05
Acalabrutinib	BTK	0.045	1000	59.91324803	0.000462513	1.61551E-05
Acalabrutinib	BTK	0.045	1000	49.92770669	0.000367588	1.62148E-05
Acalabrutinib	BTK	0.045	1000	41.60642224	0.000337013	1.39989E-05
Acalabrutinib	BTK	0.045	1000	34.67201853	0.000267423	1.35051E-05
Acalabrutinib	BTK	0.045	1000	28.89334878	0.000258543	1.29368E-05

Supplemental Figure 4. BTK enzyme kinetics plots for acalabrutinib (2)

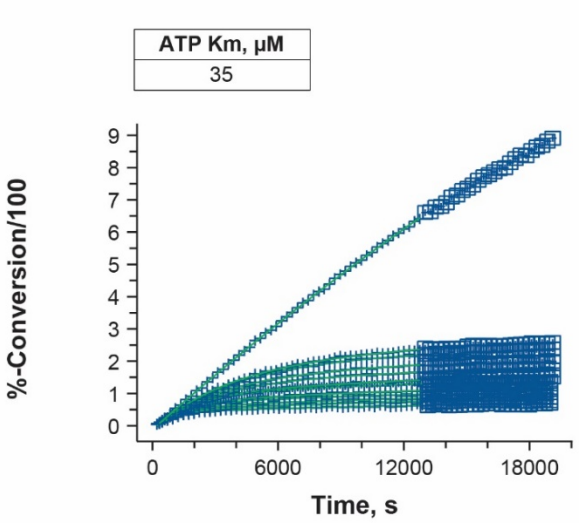

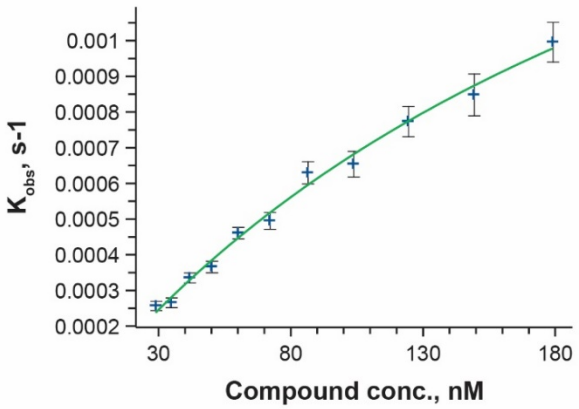

BTK (Parameter)	Value	Units
K_{inact} (K2)	0.002445156	s-1
K_{iapp} *(1+[S]/Km)	268.4275192	nM
K-2	0	s-1
K_i	9.077259104	nM
K_{inact}/K_i	0.000269372	nM-1*s-1
Residence Time (1/K-2)	Indefinite	s
FIT Statistics	**Goodness of Fit**	
Chi^2	4.48445E-09	
F-test	0.993266345	
T-test	0.919983958	

Supplemental Table 5. TEC enzyme kinetics data for ibrutinib (0.3 nM TEC)

Compound	Enzyme	Enzyme concentration, nM	ATP concentration, uM	Compound concentration, nM	K_{obs}, s-1	95%-confidence
Ibrutinib	TEC	0.3	1000	15	0.003711357	0.000325344
Ibrutinib	TEC	0.3	1000	12.5	0.003203723	0.000259978
Ibrutinib	TEC	0.3	1000	10.41666667	0.002651187	0.00019961
Ibrutinib	TEC	0.3	1000	8.680555556	0.002183536	0.00018315
Ibrutinib	TEC	0.3	1000	7.233796296	0.001448589	0.000194026
Ibrutinib	TEC	0.3	1000	6.02816358	0.001166187	6.24796E-05
Ibrutinib	TEC	0.3	1000	5.02346965	0.001551147	4.94976E-05
Ibrutinib	TEC	0.3	1000	4.186224709	0.001399701	5.60526E-05
Ibrutinib	TEC	0.3	1000	3.48852059	0.001096532	6.49649E-05
Ibrutinib	TEC	0.3	1000	2.907100492	0.001014172	7.17453E-05
Ibrutinib	TEC	0.3	1000	2.422583743	0.000728765	7.20165E-05

Supplemental Figure 5. TEC enzyme kinetics plots for ibrutinib (1)

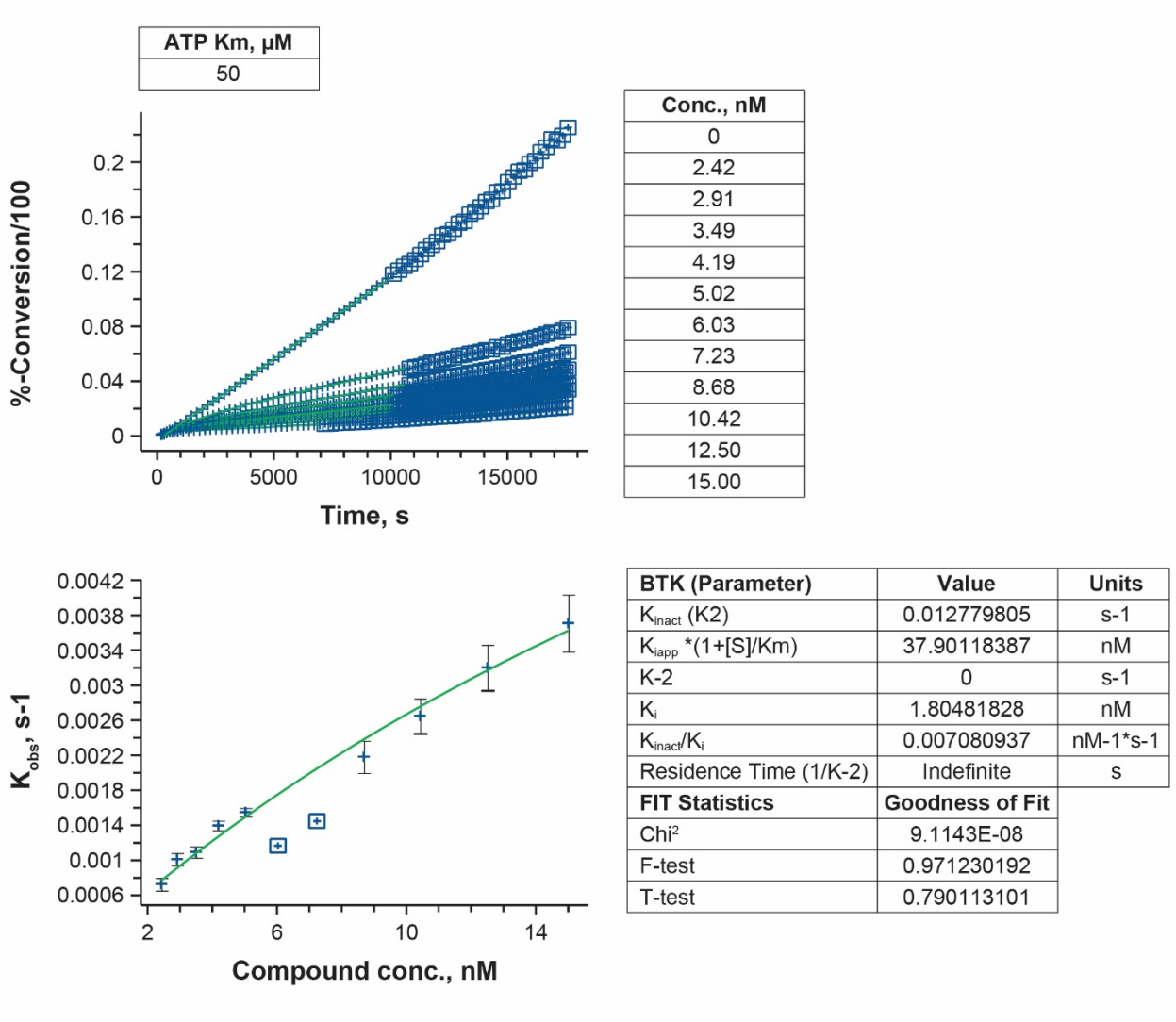

BTK (Parameter)	Value	Units
K_{inact} (K2)	0.012779805	s-1
K_{iapp} *(1+[S]/Km)	37.90118387	nM
K-2	0	s-1
K_i	1.80481828	nM
K_{inact}/K_i	0.007080937	nM-1*s-1
Residence Time (1/K-2)	Indefinite	s
FIT Statistics	**Goodness of Fit**	
Chi^2	9.1143E-08	
F-test	0.971230192	
T-test	0.790113101	

Supplemental Table 6. TEC enzyme kinetics data for ibrutinib (0.115 nM TEC)

Compound	Enzyme	Enzyme concentration, nM	ATP concentration, uM	Compound concentration, nM	K_{obs}, s-1	95%-confidence
Ibrutinib	TEC	0.115	1000	8	0.002299512	0.000361184
Ibrutinib	TEC	0.115	1000	6.666666667	0.002103881	0.000225242
Ibrutinib	TEC	0.115	1000	5.555555556	0.002239668	0.000315757
Ibrutinib	TEC	0.115	1000	4.62962963	0.001681009	0.00016689
Ibrutinib	TEC	0.115	1000	3.858024691	0.001154146	8.28214E-05
Ibrutinib	TEC	0.115	1000	3.215020576	0.000939698	6.22118E-05
Ibrutinib	TEC	0.115	1000	2.679183813	0.000944351	7.14332E-05
Ibrutinib	TEC	0.115	1000	2.232653178	0.000731845	0.000149011
Ibrutinib	TEC	0.115	1000	1.860544315	0.000551128	0.000254758
Ibrutinib	TEC	0.115	1000	1.550453596	0.000731739	0.000384208
Ibrutinib	TEC	0.115	1000	1.292044663	0.000330385	0.000190587

Supplemental Figure 6. TEC enzyme kinetics plots for ibrutinib (2)

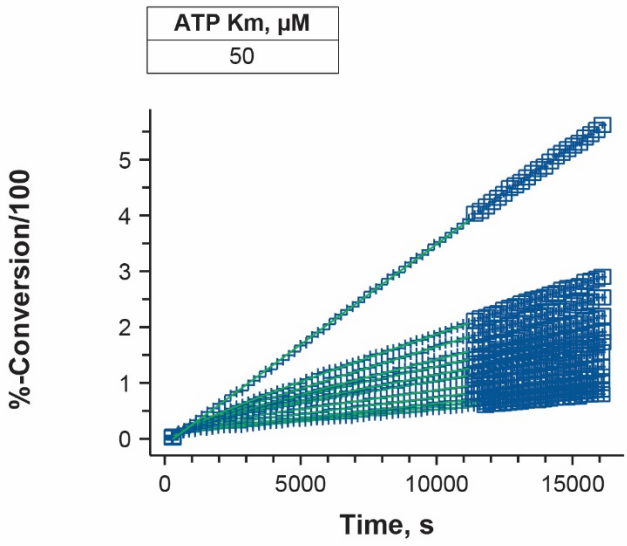

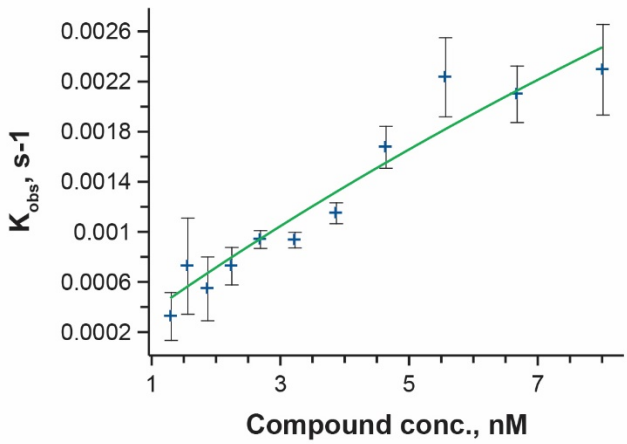

BTK (Parameter)	Value	Units
K_{inact} (K2)	0.013673896	s-1
K_{iapp} *(1+[S]/Km)	36.24299237	nM
K-2	0	s-1
K_i	1.725856779	nM
K_{inact}/K_i	0.007922961	nM-1*s-1
Residence Time (1/K-2)	Indefinite	s
FIT Statistics	**Goodness of Fit**	
Chi^2	3.48818E-07	
F-test	0.841756899	
T-test	0.85094791	

Supplemental Table 7. TEC enzyme kinetics data for acalabrutinib (0.3 nM TEC)

Compound	Enzyme	Enzyme concentration, nM	ATP concentration, uM	Compound concentration, nM	K_{obs}, s-1	95%-confidence
Acalabrutinib	TEC	0.3	1000	804.9	0.00235	0.000128222
Acalabrutinib	TEC	0.3	1000	670.75	0.001969861	0.000115078
Acalabrutinib	TEC	0.3	1000	558.9583333	0.001576885	9.46784E-05
Acalabrutinib	TEC	0.3	1000	465.7986111	0.001410129	0.000131697
Acalabrutinib	TEC	0.3	1000	388.1655093	0.00100748	8.94748E-05
Acalabrutinib	TEC	0.3	1000	323.4712577	0.000836627	5.11058E-05
Acalabrutinib	TEC	0.3	1000	269.5593814	0.000978956	5.53943E-05
Acalabrutinib	TEC	0.3	1000	224.6328179	0.000885238	5.12951E-05
Acalabrutinib	TEC	0.3	1000	187.1940149	0.000716575	4.57308E-05
Acalabrutinib	TEC	0.3	1000	155.9950124	0.000642043	6.1225E-05
Acalabrutinib	TEC	0.3	1000	129.9958437	0.000441482	4.64066E-05

Supplemental Figure 7. TEC enzyme kinetics plots for acalabrutinib (1)

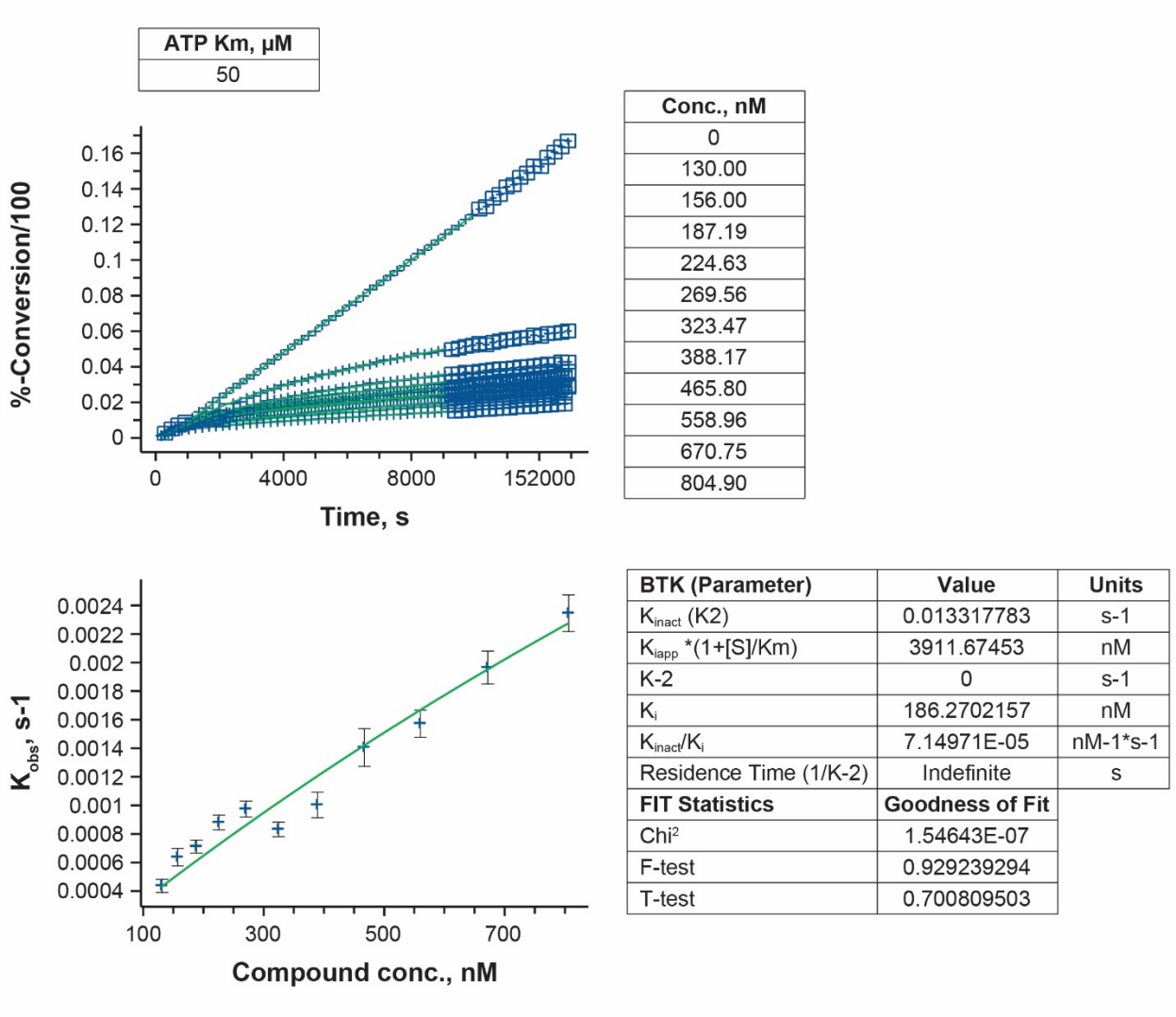

BTK (Parameter)	Value	Units
K_{inact} (K2)	0.013317783	s-1
K_{iapp} *(1+[S]/Km)	3911.67453	nM
K-2	0	s-1
K_i	186.2702157	nM
K_{inact}/K_i	7.14971E-05	nM-1*s-1
Residence Time (1/K-2)	Indefinite	s
FIT Statistics	**Goodness of Fit**	
Chi^2	1.54643E-07	
F-test	0.929239294	
T-test	0.700809503	

Supplemental Table 8. TEC enzyme kinetics data for acalabrutinib (0.2 nM TEC)

Compound	Enzyme	Enzyme concentration, nM	ATP concentration, uM	Compound concentration, nM	K_{obs}, s-1	95%-confidence
Acalabrutinib	TEC	0.2	1000	457.57	0.001630108	0.000129663
Acalabrutinib	TEC	0.2	1000	381.3083333	0.001398252	9.42539E-05
Acalabrutinib	TEC	0.2	1000	317.7569444	0.001188951	8.23696E-05
Acalabrutinib	TEC	0.2	1000	264.7974537	0.000964911	5.898E-05
Acalabrutinib	TEC	0.2	1000	220.6645448	0.000789929	5.28222E-05
Acalabrutinib	TEC	0.2	1000	183.8871206	0.000701655	3.70468E-05
Acalabrutinib	TEC	0.2	1000	153.2392672	0.000613403	2.93045E-05
Acalabrutinib	TEC	0.2	1000	127.6993893	0.000519269	2.58391E-05
Acalabrutinib	TEC	0.2	1000	106.4161578	0.000460735	2.78285E-05
Acalabrutinib	TEC	0.2	1000	88.68013148	0.000371238	2.65775E-05
Acalabrutinib	TEC	0.2	1000	73.90010956	0.00032225	2.50307E-05

Supplemental Figure 8. TEC enzyme kinetics plots for acalabrutinib (2)

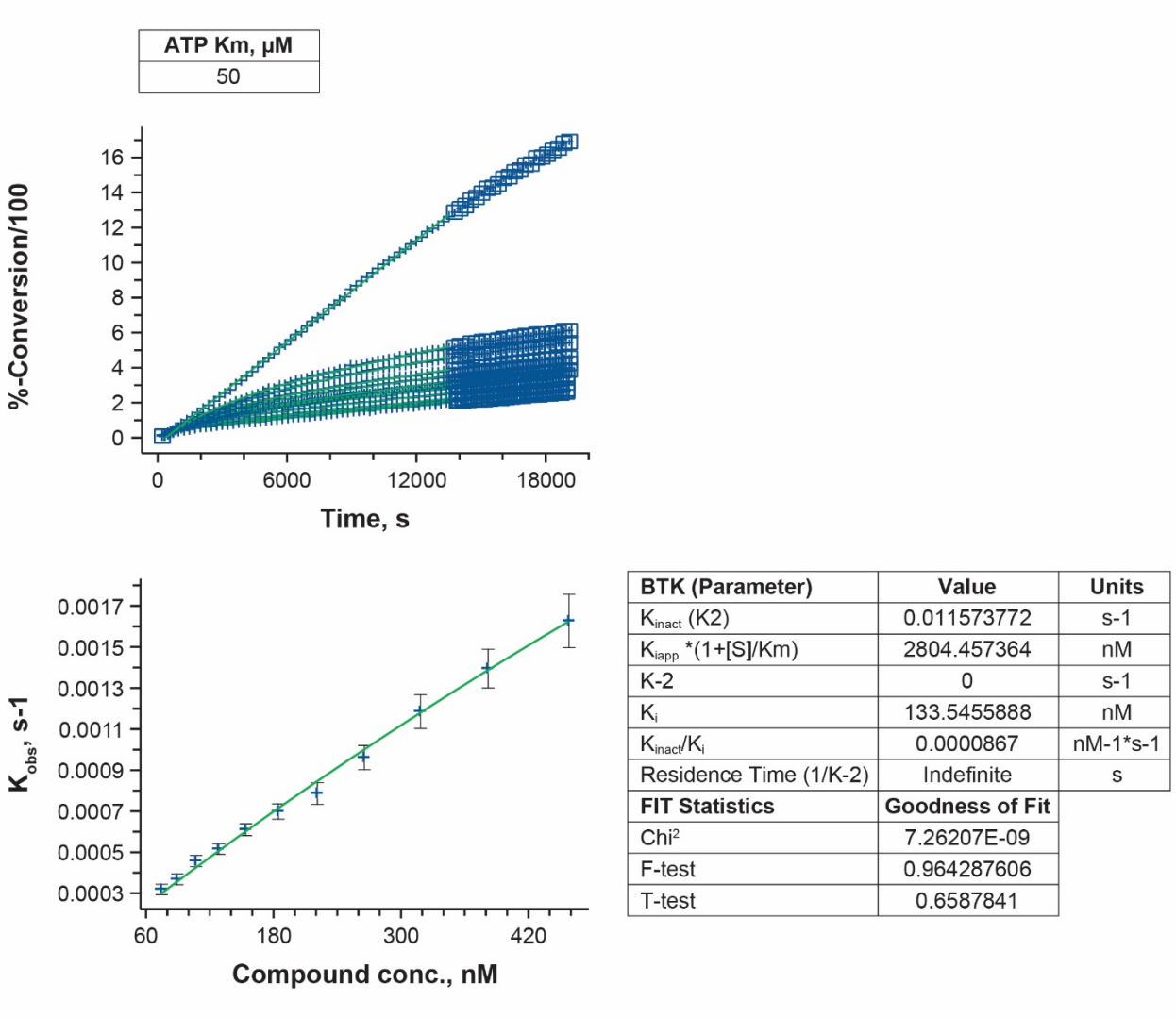

BTK (Parameter)	Value	Units
K_{inact} (K2)	0.011573772	s-1
K_{iapp} *(1+[S]/Km)	2804.457364	nM
K-2	0	s-1
K_i	133.5455888	nM
K_{inact}/K_i	0.0000867	nM-1*s-1
Residence Time (1/K-2)	Indefinite	s
FIT Statistics	**Goodness of Fit**	
Chi^2	7.26207E-09	
F-test	0.964287606	
T-test	0.6587841	